ELSEVIER

Chemical Geology 238 (2007) 1 – 18

CHEMICAL GEOLOGY
INCLUDING
ISOTOPE GEOSCIENCE

www.elsevier.com/locate/chemgeo

Noble gas and geochronology study of the Hana Ridge, Haleakala volcano, Hawaii; implications to the temporal change of magma source and the structural evolution of the submarine ridge

Takeshi Hanyu [a,*], Kevin T.M. Johnson [b], Naoto Hirano [c,1], Zhong-Yuan Ren [a]

[a] *Institute for Research on Earth Evolution, Japan Agency for Marine-Earth Science and Technology, Yokosuka, 237-0061, Japan*
[b] *Department of Geology and Geophysics, University of Hawaii at Manoa, Honolulu, HI 96822, USA*
[c] *Earth and Planetary Sciences, Tokyo Institute of Technology, Meguro, Tokyo 152-8551, Japan*

Received 22 May 2006; received in revised form 27 September 2006; accepted 27 September 2006

Editor: P. Deines

Abstract

In order to constrain the magma sources and the structural evolution of Hana Ridge, noble gas isotope ratios and $^{40}Ar/^{39}Ar$ ages were determined for this submarine extension of the east rift zone of Haleakala volcano. $^{40}Ar/^{39}Ar$ ages of ten lavas from Hana Ridge are bimodally distributed. Three samples have ages of 1.8–1.9 Ma and seven samples have ages of 1.4–1.5 Ma. The observation of older lavas overlying younger ones in two locations suggests that growth of Hawaiian rift zones occurs endogenously by continuous intrusion of magmas and patchy resurfacing at outbreak points. The 0.5 Ma age range for submarine Hana Ridge lavas, coupled with previously published K/Ar ages of 0.97–1.1 Ma for subaerial Honomanu lavas on the Haleakala Volcano, indicates that Haleakala shield volcanism persisted for nearly 1 My. Furthermore, the new $^{40}Ar/^{39}Ar$ ages, when considered with isotopic compositions of the lavas, suggests that the source for Hana Ridge magmas gradually shifted over a period of 0.5–1.0 My.

The majority of samples from the ridge have relatively uniform $^{3}He/^{4}He$ ratios between 18 and 22 Ra, which is higher than $^{3}He/^{4}He$ of subaerial Honomanu tholeiites. $^{20}Ne/^{22}Ne$ and $^{21}Ne/^{22}Ne$ ratios define linearly correlated trend that overlaps with the Loihi–Kilauea trend. He–Ne systematics of the Hana Ridge indicate that the magmas comprising most parts of the ridge were derived from a source with a primordial less-degassed mantle component. Since Hana Ridge lavas predate the subaerial Honomanu lavas, temporal decrease of $^{3}He/^{4}He$ ratios suggests that contribution of this primordial component had decreased in the magma source during establishment of Hana Ridge and Haleakala volcano. Pb–Sr isotopes demonstrate that Hana Ridge magmas are representative of the Kea component. However, such isotopic signatures associated with elevated high $^{3}He/^{4}He$ ratios precludes that the Kea component is a distinct endmember, such as recycled oceanic crust or lithospheric mantle. Alternatively, we propose that it is a common sub-component that is a mixture of Loihi endmember and recycled oceanic crust. Ne isotope ratios of the Hawaiian samples, including the Hana Ridge, show primordial signature irrespective of $^{3}He/^{4}He$ ratios. Such apparent decoupling of He and Ne isotopes may be also attributed to mixing of the Loihi component and recycled component in the mantle plume, either of which components needs to be elementally fractionated prior to mixing.

Keywords: Hawaii; Mantle plume; Submarine ridge; Noble gas; $^{40}Ar/^{39}Ar$ dating

* Corresponding author. Tel.: +81 46 867 9807; fax: +81 46 867 9625.
E-mail address: hanyut@jamstec.go.jp (T. Hanyu).
[1] Present address: Scripps Institution of Oceanography, University of California, San Diego, La Jolla, CA 92093-0225, USA.

0009-2541/$ - see front matter © 2006 Elsevier B.V. All rights reserved.
doi:10.1016/j.chemgeo.2006.09.008

1. Introduction

Hawaii has been recognized as one of the largest hotspots related to an upwelling mantle plume originating from the deep mantle (Davies, 1988; Sleep, 1990; Courtillot et al., 2003). Extensive production of magma induces both submarine and subaerial eruption, establishing a chain of volcanic islands on a moving oceanic plate. Petrological and geochemical studies have demonstrated that the source compositions and melting processes of the mantle plume change during volcano growth among pre-shield stage, shield stage, post-shield stage and rejuvenated stage (Chen and Frey, 1985; Stille et al., 1986; Clague and Dalrymple, 1987; Kurz and Kammer, 1991; Ren et al., 2004; Abouchami et al., 2005; Bryce et al., 2005; Ren et al., 2006). However, this evolutionary trend is not yet fully understood, particularly for the early stage of volcano growth, because the late stage lavas cover the surface of the volcano, hiding the volcanic body established during the early stage.

In order to address this problem, the Hawaiian Scientific Drilling Project was initiated and has yielded important information on the temporal change of magma compositions with very high stratigraphic resolution (Stolper et al., 1996; Bryce et al., 2005). These new data have helped to constrain new models of heterogeneous structure of the Hawaiian mantle plume (Hauri et al., 1996; Kurz et al., 1996; Lassiter et al., 1996; DePaolo et al., 2001; Blichert-Toft et al., 2003; Eisele et al., 2003; Kurz et al., 2004; Abouchami et al., 2005; Bryce et al., 2005). Coupled with the HSDP results, recent underwater surveys have revealed magmatic activity in the submarine part of the volcanic edifice (e.g., Naka and Team, 2000), such as ancestral portions of the shield volcanism exposed by landslide, submarine ridges, arch volcanism and alkalic lava fields distributed widely around the main shield volcanoes (Takahashi et al. (2002) and papers therein). Results from these surveys should also provide new information on the entire volcanic system at the hotspot.

Rift zones are major expressions of Hawaiian volcanism. Hawaiian shield volcanoes are fed from a central magma chamber beneath the summit, followed by magma transport underground from its source along the rift zone (Tilling and Dvorak, 1993). Many submarine ridges in Hawaii are extensions of subaerial rift zones and can preserve information of early stages of the shield growth as more centrally erupted lavas may be covered by post-shield and rejuvenated stage lavas. Here we present new noble gas data and $^{40}Ar/^{39}Ar$ ages

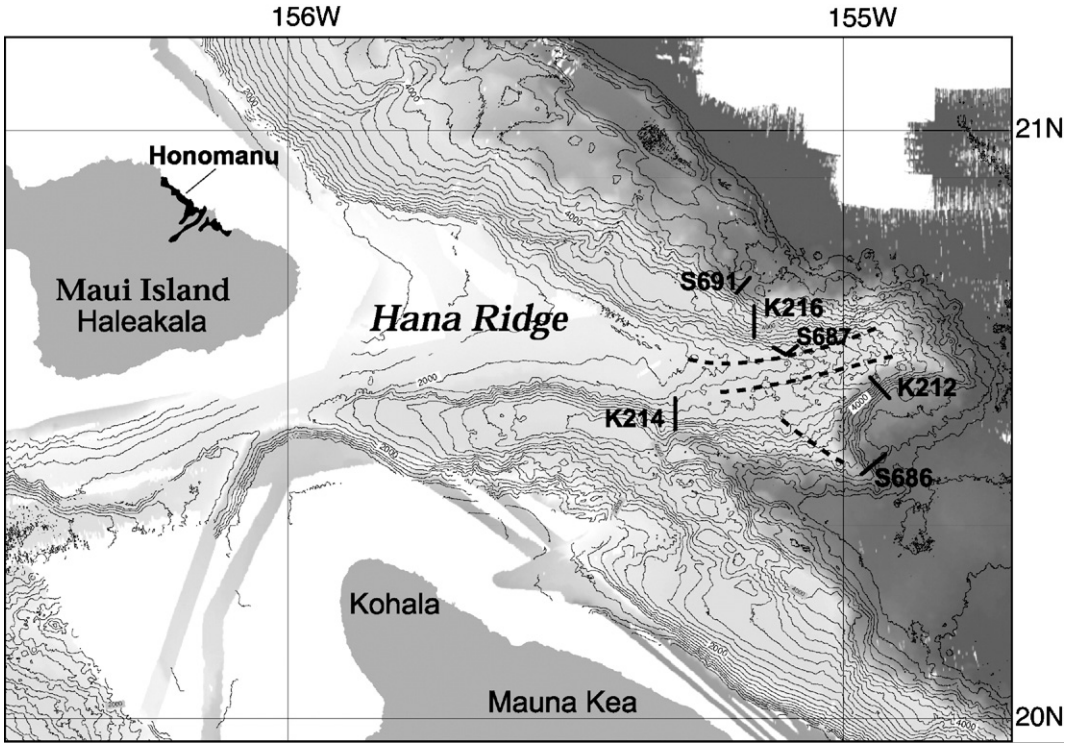

Fig. 1. Map of the Halaeakala Volcano and the Hana Ridge. The dive sites and dive tracks are shown by solid lines. Dotted lines indicate structural lineaments. Honomanu tholeiites on the Maui Island is the only exposure of the shield stage lavas at the Haleakala Volcano.

from the Hana Ridge, a submarine rift zone of the Haleakala volcano. This ridge was surveyed during the scientific cruises conducted by Japan Agency for Marine-Earth Science and Technology (JAMSTEC) in 2001 and 2002. Although several geophysical and geological data sets had been obtained prior to this survey (Malahoff and Woollard, 1968; Moore et al., 1990; Clague et al., 2000), direct observation and extensive rock collection using submersibles during the survey enhanced understanding of the detailed morphology and the magma composition of the ridge (Smith et al., 2002; Ren et al., 2004, 2006). The purpose of this study is to further constrain the magma source and its temporal change in compositions during growth of the volcano. Noble gas data presented in this study will also provide better understanding of structural evolution during establishment of the ridge and its relationships to the magmatic activity at the central shield volcano.

2. Geological background and samples

Hana Ridge is the east-southeast trending submarine extension of the east rift zone of Haleakala volcano on the island of Maui (Fig. 1). It is 5500 m deep at its eastern terminus and is 140 km long, making it the largest submarine ridge among the Hawaiian volcanoes. The underwater surveys reveal that the ridge has complex geometry and morphology (Smith et al., 2002). The slopes of Hana Ridge mostly consist of intact and broken pillow lavas, lobate and sheet flows and rock fragments. There are numerous flat-topped volcanic cones on the eastern part of the ridge (Clague et al., 2000). In contrast, the western half of the ridge has a relatively flat surface covered by corals down to ~2000 m depth, suggesting that the ridge experienced subsidence after reef building (Moore et al., 1990). In the eastern half of the ridge, there are major structural lineaments that are defined by bathymetry and backscatter image. The eastern terminus of Hana Ridge contains a unique amphitheater-shaped structure (Fig. 1) that might be formed by a landslide or by branched construction of volcanism (Smith et al., 2002), the former of which has been suggested by the geophysical surveys (Eakins and Robinson, 2006). The $^{234}U/^{238}U$ age of the coral cap on the western portion of Hana Ridge is 0.85 Ma (Moore and Campbell, 1987) and 0.75 Ma (Moore et al., 1990). K–Ar ages of subaerial Honomamu series lavas exposed on the Haleakala volcano range from 1.1 to 0.97 Ma (Chen et al., 1991).

Table 1
Sample description

Sample name	Location			Rock type
	Latitute	Longitude	Depth (m)	
K212-2A	20° 32.56′ N	154° 56.26′ W	4747	Picritic basalt
K212-3A	20° 32.66′ N	154° 56.33′ W	4568	Olivine basalt
K212-4	20° 32.80′ N	154° 56.41′ W	4496	Olivine basalt
K212-6B	20° 32.89′ N	154° 56.45′ W	4402	Olivine basalt
K212-13B	20° 33.61′ N	154° 57.01′ W	3619	Olivine basalt
K214-3	20° 28.35′ N	155° 16.06′ W	4332	Picritic basalt
K214-5B	20° 28.47′ N	155° 16.08′ W	4251	Olivine basalt
K214-7	20° 28.71′ N	155° 16.07′ W	4095	Olivine-plagioclase basalt
K214-10	20° 28.96′ N	155° 16.09′ W	3856	Olivine-plagioclase basalt
K214-9	20° 28.87′ N	155° 16.07′ W	3948	Picritic basalt
K214-13	20° 29.44′ N	155° 16.01′ W	3584	Olivine basalt
K214-15A	20° 30.17′ N	155° 15.93′ W	3174	Picritic basalt
K214-15D	20° 30.17′ N	155° 15.93′ W	3174	Picritic basalt
K216-3	20° 38.19′ N	155° 08.02′ W	2913	Olivine basalt
K216-4	20° 38.19′ N	155° 08.06′ W	2807	Olivine basalt
K216-8A	20° 37.63′ N	155° 08.12′ W	2505	Olivine basalt
K216-10	20° 36.83′ N	155° 08.18′ W	2519	Olivine basalt
S686-1	20° 26.55′ N	154° 56.03′ W	5166	Olivine basalt
S686-2A	20° 26.32′ N	154° 56.07′ W	5032	Olivine basalt
S686-3A	20° 25.67′ N	154° 56.79′ W	4895	Olivine basalt
S687-5	20° 35.11′ N	155° 05.77′ W	2532	Olivine basalt
S687-7	20° 35.12′ N	155° 05.87′ W	2462	Olivine basalt
S687-11	20° 35.06′ N	155° 06.09′ W	2411	Picritic basalt
S691-2A	20° 40.80′ N	155° 07.37′ W	4303	Olivine-plagioclase basalt
S691-3	20° 40.48′ N	155° 07.57′ W	4146	Olivine basalt
S691-5A	20° 39.94′ N	155° 07.93′ W	3788	Olivine basalt

Table 2
Noble gas abundances and isotope ratios by crushing extraction

Sample	Weight	Crushing times	Abundance (cm^3 STP/g)					Isotope ratios										
	(g)		^{4}He	^{20}Ne	^{36}Ar	^{84}Kr	^{132}Xe	^{3}He/^{4}He	Error	^{20}Ne/^{22}Ne	Error	^{21}Ne/^{22}Ne	Error	^{38}Ar/^{36}Ar	Error	^{40}Ar/^{36}Ar	Error	^{4}He/^{40}Ar*
			(10^{-9})	(10^{-12})	(10^{-12})	(10^{-12})	(10^{-12})	(R/Ra)[a]	(1σ)		(1σ)		(1σ)		(1σ)		(1σ)	
K212-2A	1.183	100	11.9	86.0	31.6	0.82	0.078	20.6	0.3	9.99	0.09	0.0300	0.0010	0.1883	0.0007	809.0	4.1	0.73
K212-4	1.040	100	6.75	257	16.6	0.40	0.049	22.4	0.4	9.82	0.07	0.0286	0.0007	0.1886	0.0012	492.1	2.5	2.07
K212-6B	0.943	100	13.9	98.4	17.0	1.38	0.034	18.9	0.5	10.15	0.06	0.0301	0.0009	0.1884	0.0011	535.9	8.8	3.39
K214-3	0.596	100	10.7	118	20.0	0.54	0.072	19.4	0.5	10.01	0.08	0.0296	0.0011	0.1879	0.0012	857.8	4.4	0.95
K214-5B	1.514	100	24.1	50.2	18.1	1.82	0.032	18.6	0.3	10.57	0.07	0.0319	0.0010	0.1883	0.0009	2049	34	0.76
K214-7	0.633	100	4.94	81.3	9.5	2.47	0.033	20.7	0.8	10.05	0.07	0.0312	0.0011	0.1875	0.0020	386.8	6.4	5.69
K214-9	1.377	100	16.6	116	28.8	0.77	0.066	12.3	0.2	9.76	0.07	0.0288	0.0009	0.1873	0.0009	502.1	2.6	2.79
K214-13	0.818	100	6.40	120	22.6	3.20	0.027	19.5	0.5	10.08	0.06	0.0301	0.0007	0.1885	0.0016	515.8	8.5	1.29
K214-15A	1.700	30	10.4	90.3	15.2	0.29	0.030	15.0	0.3	9.78	0.06	0.0292	0.0009	0.1883	0.0009	1007	5	0.96
(Stepwise)		70	3.98	67.2	8.9	0.23	0.020	13.8	0.4	9.84	0.08	0.0298	0.0009	0.1881	0.0010	551.1	2.8	1.76
K214-15D	1.914	100	19.6	204	230	4.76	0.097	13.0	0.3	9.87	0.05	0.0293	0.0005	0.1875	0.0005	377.0	6.2	1.04
K216-4	0.397	100	17.1	177	19.9	2.08	0.050	18.9	0.7	10.16	0.06	0.0306	0.0008	0.1892	0.0020	1844	30	0.55
K216-8A	0.330	100	6.22	271	118	5.72	0.10	18.1	1.1	10.01	0.07	0.0301	0.0004	0.1885	0.0008	362.4	6.0	0.79
S686-1	1.303	100	13.7	82.0	44.2	3.57	0.048	19.3	0.4	10.37	0.07	0.0306	0.0007	0.1887	0.0007	1210	20	0.34
S686-3A	0.700	100	7.83	122	15.1	0.43	0.072	20.5	0.5	9.88	0.10	0.0295	0.0011	0.1887	0.0016	1032	5	0.70
S687-7	0.501	100	4.82	99.6	21.0	0.54	0.052	18.3	0.7	9.87	0.11	0.0297	0.0011	0.1882	0.0011	991.3	5.2	0.33
S687-11	0.740	100	8.66	180	60.7	4.96	0.057	18.6	0.7	9.94	0.06	0.0296	0.0005	0.1890	0.0007	480.2	8.0	0.77
S691-3	1.175	100	1.77	125	22.6	0.52	0.053	20.5	1.0	9.84	0.07	0.0289	0.0007	0.1875	0.0009	583.3	2.9	0.27
S691-5A	1.398	30	10.7	35.5	9.82	0.39	0.051	19.0	0.3	10.32	0.09	0.0315	0.0011	0.1890	0.0018	2700	15	0.45
(Stepwise)		70	4.30	34.8	8.30	0.27	0.049	19.5	0.5	10.87	0.14	0.0318	0.0010	0.1894	0.0015	2414	13	0.24
Typical blank			0.001	3	1	0.003	0.005											

[a]He isotope ratios are normalized by atmospheric value (1.40×10^{-6}).

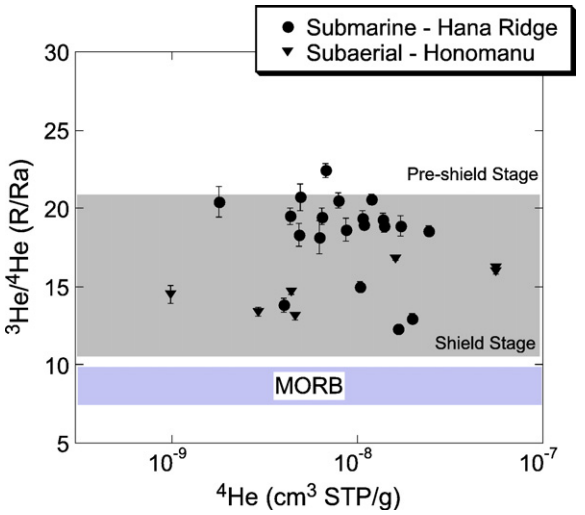

Fig. 2. ^{3}He/^{4}He ratios versus ^{4}He concentration for the Hana Ridge samples. ^{3}He/^{4}He ratios are normalized to the atmospheric ratio. Data for subaerial Honomanu tholeiites are also shown (Kurz et al., 1987). Typical range of ^{3}He/^{4}He ratios for MORB, shield stage and pre-shield stage is shown by hatches.

Field observations and rock collection were carried out using remotely operated vehicle Kaiko and manned submersible Shinkai 6500 during the scientific cruises by JAMSTEC in 2001 and 2002. The dive sites were designed to survey the distal eastern half of the ridge, including northern and southern slopes and eastern amphitheater shaped wall, and to collect stratigraphic sections of lavas comprising the ridge (Fig. 1). Kaiko visited three sites in 2001 (K212, K214, K216), and another three dives were conducted with Shinkai 6500 in 2002 (S686, S687, S691). The purpose of dives K212 and S686 were to observe the slope of the amphitheater-shaped wall at the tip of the ridge. In dive K214, we traced the lower two thirds of the southern flank. Dives K216 and S687 targeted the upper slope of the ridge and some flat-topped volcanic cones. Dive S691 was designed to survey the lower part of the northern flank. Detailed sample information, including specific sample localities and whole rock geochemistry, has been presented elsewhere (Ren et al., 2004, 2005).

Description of samples used in this study is shown in Table 1. The recovered rocks are tholeiitic basalts that have variable mineral modal compositions, including olivine basalts and picritic basalts. Olivine dominates among phenocrysts in most samples, but some samples contain augite +/− plagioclase and orthopyroxene. Ren et al. (2004) showed that there are three types of olivines in the Hana Ridge basalts, including euhedral, subhedral-undeformed and deformed olivine phenocrysts, suggesting that some olivines may originate from accumulation in a magma chamber deformed during eruption. The Mg# of olivines ranges from 0.82 and 0.91. They found that all olivines, regardless of textural

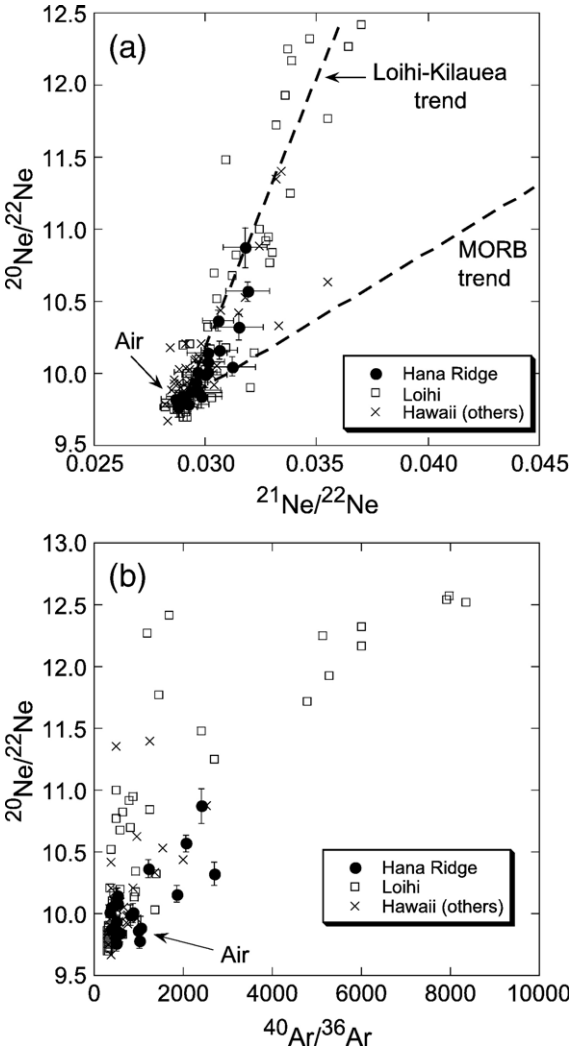

Fig. 3. (a) Ne-three isotope diagram for the Hana Ridge samples. These data define a linear trend that overlaps with the Loihi–Kilauea trend (Honda et al., 1991). The data sources for Loihi, Kilauea, Mauna Kea, Hualalai and samples obtained by Hawaii Scientific Drilling Project are Sarda et al. (1988), Honda et al. (1991), Hiyagon et al. (1992), Honda et al. (1993b), Valbracht et al. (1997), Trieloff et al. (2000) and Althaus et al. (2003). (b) ^{20}Ne/^{22}Ne against ^{40}Ar/^{36}Ar for the Hana Ridge and other Hawaiian samples. The data sources are the same as those in (a). The samples associated with higher ^{20}Ne/^{22}Ne than atmospheric ratio show elevated ^{40}Ar/^{36}Ar and the Ne–Ar systematics is best explained by two component mixing between the magmatic endmember and air. Extrapolating the trend toward the assumed primordial mantle ^{20}Ne/^{22}Ne value of 12.5 (Ne–B) or 13.8 (Solar) enables the estimation of its ^{40}Ar/^{36}Ar of 6000 or higher, which is consistent with the previous studies (Trieloff et al., 2000).

type, have CaO contents typical of magmatic olivine and significantly higher than that of mantle (i.e., xenocrystic) olivine. They further indicated that melt inclusions in those olivines define a compositional trend similar to whole rocks. These observations led the authors to conclude that all olivines were crystallized from the magma. The basalts from submarine Hana Ridge and subaerial Honomanu tholeiites on Haleakala have distinct major and trace element compositions. Most submarine Hana Ridge samples overlap Kilauea lavas in major and trace element and Sr–Nd–Pb isotopic compositions, whereas Honomanu tholeiites have compositions intermediate between Kilauea and Mauna Loa or similar to Mauna Loa lavas, suggesting different primary magmas or different source components (Ren et al., 2004, 2006).

Olivine phenocrysts and whole rock samples were used for noble gas analyses and $^{40}Ar/^{39}Ar$ dating, respectively. Analyses for noble gases were conducted at JAMSTEC by crushing and heating extraction techniques. $^{40}Ar/^{39}Ar$ age determination was performed at Oregon State University and University of Tokyo. Details of experimental methods are described in Appendix.

3. Results

3.1. Crushing experiments

Results for crushing experiments are shown in Table 2. Stepwise crushing test was performed on two samples (K214-15A and S691-5A) to assess if in-situ radiogenic component, particularly ^4He produced by U and Th decay, might alter isotopic ratios by extended crushing strokes. We note that a cosmogenic component is negligible as the samples were emplaced and resided in a submarine setting. Greater amount of ^4He was extracted in the first step (30 strokes) than in the second step (70 strokes) for both samples. $^3He/^4He$ ratios in the first and second steps were comparable to each other at the 2σ uncertainty level.

$^3He/^4He$ ratios are plotted against ^4He concentrations in Fig. 2. Most of the samples have $^3He/^4He$ ratios between 18.1 and 22.4 Ra. These data do not show systematic correlation between $^3He/^4He$ ratios and ^4He concentrations, suggesting that in-situ radiogenic component is negligible for the crushing data. Exceptions are K214-9, K214-15A and K214-15D, having distinctly low $^3He/^4He$ compared to the other samples. These three samples have almost equivalent $^3He/^4He$ ratios as the subaerial Honomanu tholeiites (Fig. 2).

Several samples show elevated $^{20}Ne/^{22}Ne$ and $^{21}Ne/^{22}Ne$ ratios in comparison with atmospheric values

Table 3
Noble gas abundances and isotope ratios by heating extraction

Sample	Weight	Temperature	Abundance (cm^3STP/g)					Isotope ratios									
	(g)		^4He	^{20}Ne	^{36}Ar	^{84}Kr	^{132}Xe	$^3He/^4He$	Error	$^{20}Ne/^{22}Ne$	Error	$^{21}Ne/^{22}Ne$	Error	$^{38}Ar/^{36}Ar$	Error	$^{40}Ar/^{36}Ar$	Error	$^4He/^{40}Ar^*$
			(10^{-9})	(10^{-12})	(10^{-12})	(10^{-12})	(10^{-12})	(R/Ra)[a]	(1σ)		(1σ)		(1σ)		(1σ)		(1σ)	
K212-2A	1.010	800	2.83	188	3020	1.75	0.26	7.92	0.36	9.84	0.05	0.0291	0.0004	0.1886	0.0003	302.0	5.0	0.14
		1850	10.7	167	733	5.95	0.43	20.32	0.59	10.14	0.06	0.0293	0.0005	0.1881	0.0003	318.7	5.2	0.63
K212-4	0.910	800	1.36	392	1220	0.86	0.12	7.29	0.58	9.79	0.05	0.0292	0.0004	0.1885	0.0003	302.0	5.0	0.17
		1850	11.7	151	367	4.03	0.19	21.74	0.56	10.21	0.06	0.0296	0.0006	0.1880	0.0004	318.7	5.2	1.37
S686-1	0.328	800		71	1840	1.34	0.19							0.1887	0.0003	310.5	5.1	
		1850	14.5	210	360	5.22	0.24	17.81	0.61	10.15	0.07	0.0294	0.0008	0.1881	0.0004	377.1	6.2	0.49
S691-5A	1.049	800	2.96	158	2280	1.79	0.31	12.55	0.79	9.91	0.06	0.0295	0.0005	0.1885	0.0003	312.6	5.1	0.08
		1850	17.4	219	586	5.99	0.35	18.39	0.39	10.09	0.06	0.0298	0.0004	0.1881	0.0004	386.6	6.3	0.33
Typical blank		800	0.2	2	2	0.04	0.01											
		1850	0.1	4	5	0.2	0.03											

[a]He isotope ratios are normalized by atmospheric value (1.40×10^{-6}).

(Table 2). Although the maximum $^{20}Ne/^{22}Ne$ ratio among the measured samples is 10.9, which is much less than the mantle endmember value of 12.5 (Neon-B) or 13.8 (Solar), these data establish a clear correlation trend between $^{20}Ne/^{22}Ne$ and $^{21}Ne/^{22}Ne$ ratios that overlaps with the Loihi–Kilauea trend (Honda et al., 1991) (Fig. 3). $^{40}Ar/^{36}Ar$ ratios range from atmospheric value up to 2700. Samples with elevated $^{20}Ne/^{22}Ne$ ratio

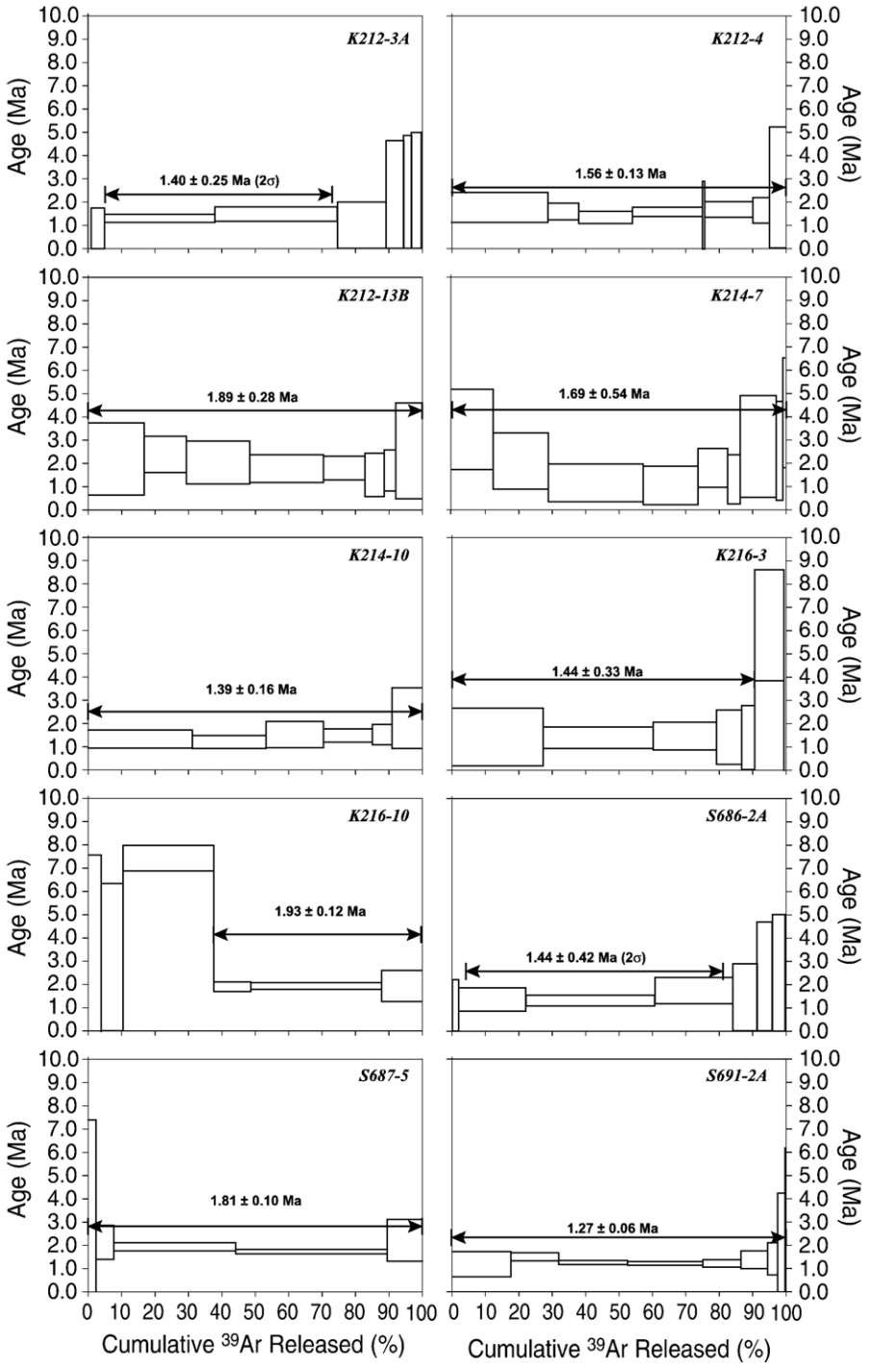

Fig. 4. Incremental heating $^{40}Ar/^{39}Ar$ analyses for the studied samples. The plateau ages, inverse isochron ages and total fusion ages are shown in Table 4. The reported errors are in 2σ level.

show relatively high $^{40}Ar/^{36}Ar$ and tend to have low Ne and Ar concentrations (Fig. 3, Table 3). These Ne–Ar systematics are principally explained by mixing of a magmatic component and an atmospheric contaminant.

Xe isotope ratios were measured for some selected samples. They were indistinguishable from atmospheric ratios, thus not shown in the tables.

$^4He/^{40}Ar^*$ ratios ($^{40}Ar^* = (^{40}Ar/^{36}Ar - 295.5) \times (^{36}Ar)$) are often used to assess noble gas fractionation from the mantle source. Some samples having relatively low $^{40}Ar/^{36}Ar$ ratios apparently show elevated $^4He/^{40}Ar^*$ presumably because $^{40}Ar^*$ was not reasonably determined due to large atmospheric contamination (Table 2). The samples with $^{40}Ar/^{36}Ar$ greater than 600 show $^4He/^{40}Ar^*$ between 0.2 and 1. This value is lower than the mantle production ratio that is defined by the mantle K/U and Th/U ratio of 10^4 and 3.3, respectively.

3.2. Heating experiments

Four samples were chosen for heating experiments (Table 3). Among the samples, greater amount of helium was extracted in the high temperature fraction (1850 °C) than in the low temperature fraction (800 °C). $^3He/^4He$ ratios in the low temperature fraction are lower than those in the high temperature fraction, suggesting that in-situ radiogenic ^4He was outgassed at 800 °C. $^3He/^4He$ ratios in the high temperature fraction are comparable to, but slightly lower than those determined by crushing experiments. This may also indicate small contribution of radiogenic ^4He in the high temperature fraction. The samples do not show large excess in $^{20}Ne/^{22}Ne$ and $^{40}Ar/^{36}Ar$ ratios, presumably due to large contribution of atmospheric component in the gases extracted in the heating experiments. Consequently, data obtained by crushing experiments will be used in the discussion below.

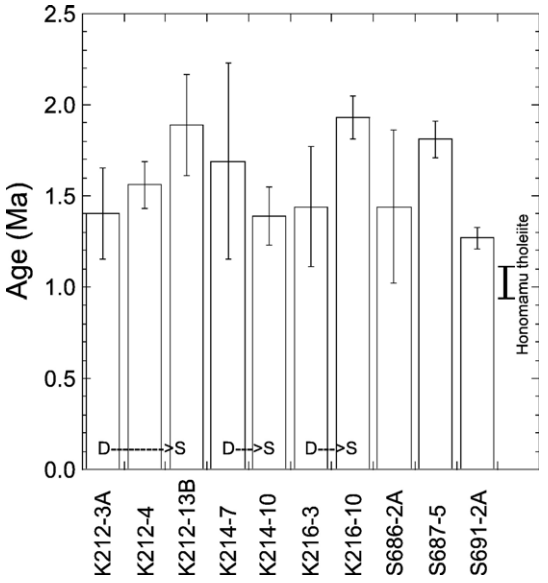

Fig. 5. Histogram of $^{40}Ar/^{39}Ar$ ages of Hana Ridge basalts collected from six dives. D = sample from deep portion of a dive, S = samples from shallow portion of a dive. Error bars are 2σ.

3.3. $^{40}Ar/^{39}Ar$ ages

Mass spectrometric data are presented graphically in Fig. 4 and summarized in Table 4. There appear to be two age groups represented by the data (Fig. 5). Most samples (from dives K212, K214, K216, S686 and S691) have ages of approximately 1.2–1.7 Ma, with a mean age of about 1.4 Ma, but three samples, K212-13B, K216-10 and S687-5, have older ages around 1.8–1.9 Ma.

Interestingly, two of these samples (K212-13B and K216-10) were collected above samples with younger ages on their respective dives. Sample K212-13B, collected at 3619 m depth at the top of the dive track,

Table 4
$^{40}Ar/^{39}Ar$ data of Hana Ridge samples

Sample	Total N	Age spectrum			Inverse isochron analysis			Total fusion
		Age±2σ	^{39}Ar	N	Age±1σ	$^{40}Ar/^{36}Ar$	N	Age±1σ
		Ma	%		Ma	Intercept		Ma
K212-3A	9	1.40±0.25	69.8	2	1.55±0.36	291.0±5.4	7	1.22±0.72
K212-4	8	1.56±0.13	100	8	1.52±0.27	296.5±5.2	8	1.67±0.24
K212-13B	9	1.89±0.28	100	9	1.52±0.69	298.2±5.3	9	2.02±0.40
K214-7	10	1.69±0.54	100	10	0.32±0.22	303.1±4.8	10	1.89±0.47
K214-10	7	1.39±0.16	100	7	1.33±0.36	296.8±7.0	7	1.46±0.21
K216-3	7	1.44±0.33	90.9	5	1.43±0.93	295.6±6.8	5	1.86±0.46
K216-10	7	1.93±0.12	62.4	3	1.91±0.14	297.1±3.7	5	3.48±0.33
S686-2A	9	1.44±0.42	82.1	3	1.32±0.24	296.1±3.2	9	1.15±0.62
S687-5	6	1.81±0.10	100	6	1.74±0.11	300.9±5.0	6	1.92±0.17
S691-2A	9	1.27±0.06	100	9	1.22±0.10	298.4±4.3	9	1.31±0.12

has an age of 1.89±0.28 Ma, while samples K212-3A (4568 m) and K212-4 (4496 m) have ages of 1.40±0.25 and 1.56±0.13 Ma, respectively. The ages of samples K212-4 and K212-13B overlap within analytical uncertainty at 1.6–1.7 Ma, but the maximum age of sample K212-3A is lower by 0.08 Ma than the minimum age of K212-13B, considering 2σ uncertainty. Another of the older samples, K216-10 (2519 m depth), has an age of 1.93±0.12 Ma. This age is greater than that of the deeper sample, K216-3 (1.44±0.33 Ma; 2913 m depth), analyzed from this dive.

The third sample in the older group, S687-5 (1.81±0.10 Ma), is the only dated sample from this dive. The dive is located on the flank of a flat topped edifice near the crest of the Hana Ridge at a depth of 2532 m. As such, it is expected to be one of the younger features on the ridge, so its 1.81 Ma age is surprising.

4. Discussion

4.1. Variation of He isotope ratios of the submarine Hana Ridge and the subaerial Honomanu of Haleakala shield

Helium isotopes have been widely used to assess contribution of the less-degassed component that presumably resides in the deep mantle. Most of the pre-shield stage and shield stage magmas in Hawaii have higher $^{3}He/^{4}He$ ratios than the depleted MORB source mantle, which leads to the idea that the Hawaiian plume involves a significant amount of the less-degassed component (Rison and Craig, 1983; Kaneoka et al., 1983; Kurz et al., 1983; Sarda et al., 1988; Kurz and Kammer, 1991; Hiyagon et al., 1992; Honda et al., 1993b; Valbracht et al., 1997; Trieloff et al., 2000; Kurz et al., 2004). This study enables us to understand how contribution from the less-degassed mantle changed in the magma source during growth of a volcano, because $^{40}Ar/^{39}Ar$ dating demonstrates that the Hana Ridge samples record the magma compositions in the early stage of shield growth (1.3–1.9 Ma), in comparison to Honomanu tholeiites (0.97–1.1 Ma; Chen et al., 1991).

The samples from the dive sites of K212, K216, S686, S687 and S691 have uniform and higher $^{3}He/^{4}He$ ratios than the subaerial Honomanu tholeiites (Table 2, Fig. 2). The samples from K214 show binary $^{3}He/^{4}He$ ratios. K214-3, K214-5B, K214-7 and K214-13 have similar $^{3}He/^{4}He$ to the samples collected from the other dive sites. In contrast, K214-9, K214-15A and K214-15D show comparable $^{3}He/^{4}He$ to subaerial Honomanu tholeiites (Kurz et al., 1987). This may indicate that the basalts from the K214 site have various origins.

The K214 dive track was designed to observe the southern flank of the Hana Ridge from the base to the top (Fig. 1). In the lower half of the ridge edifice, we observed lobate lava flows, pillow lavas and pillow breccias that were mostly in-situ erupted lavas, indicating that the lower part is composed of submarine erupted lavas. In contrast, no in-situ pillow lavas were found on the upper part of the ridge (above-3400 m), and the slope was filled with talus blocks. Samples K214-15A and K214-15D were rounded basalt cobbles collected on the upper slope, and appeared to be rounded by shallow water wave action. Taking their relatively low $^{3}He/^{4}He$ ratios into consideration, they were presumably subaerial or shallow erupted submarine lava blocks that were derived from lavas similar to the subaerial Honomamu tholeiites and moved down the slope. There is no geological implication that the K214-9 sample was also subaerial lava, but the field observation rather suggests that it was in-situ pillow lava.

Pb isotope ratios provide additional information for their origin. Ren et al. (2006) have reported that $^{206}Pb/^{204}Pb$ ratios range between 18.50 and 18.69 for most of the samples from K212, K214 and K216 sites and are similar to Kilauea lavas. However, the exceptions are K214-9 and K214-15A samples that have $^{206}Pb/^{204}Pb$ of 18.34 and 18.38, respectively (no Pb isotopic data available for K214-15D), overlapping the Pb isotope ratios of subaerial Honomamu tholeiites (Ren et al., 2006) (Fig. 6). Consequently, He–Pb isotopes strongly demonstrate that the magma source of the three samples from the K214 site differed from that of the other samples from the Hana Ridge.

4.2. Early stage magma sources of Haleakala and origin of Kea component

He isotope ratios and their variability, coupled with Pb–Sr–Nd isotopes, have been used to identify the source components responsible for generating the source magmas (e.g., Staudigel et al., 1984; West and Leeman, 1987; Frey and Rhodes, 1993; Lassiter and Hauri, 1998; Blichert-Toft et al., 2003; Ren et al., 2006). One component, characterized by high $^{87}Sr/^{86}Sr$ and low $^{206}Pb/^{204}Pb$ and $^{143}Nd/^{144}Nd$, is best represented by lavas from Koolau (Makapuu stage) volcano; referred as "Koolau" component. The other component, with low $^{87}Sr/^{86}Sr$ and high $^{206}Pb/^{204}Pb$ and $^{143}Nd/^{144}Nd$, is represented by lavas from Kilauea volcano and it is termed "Kea" component. A third component, clearly identified by Loihi lavas, is required to account for high $^{3}He/^{4}He$ (Kurz et al., 1995; Eiler et al., 1996; Hauri et al., 1996).

The Loihi samples have large variation in isotope ratios that is principally explained by mixing of "Loihi"

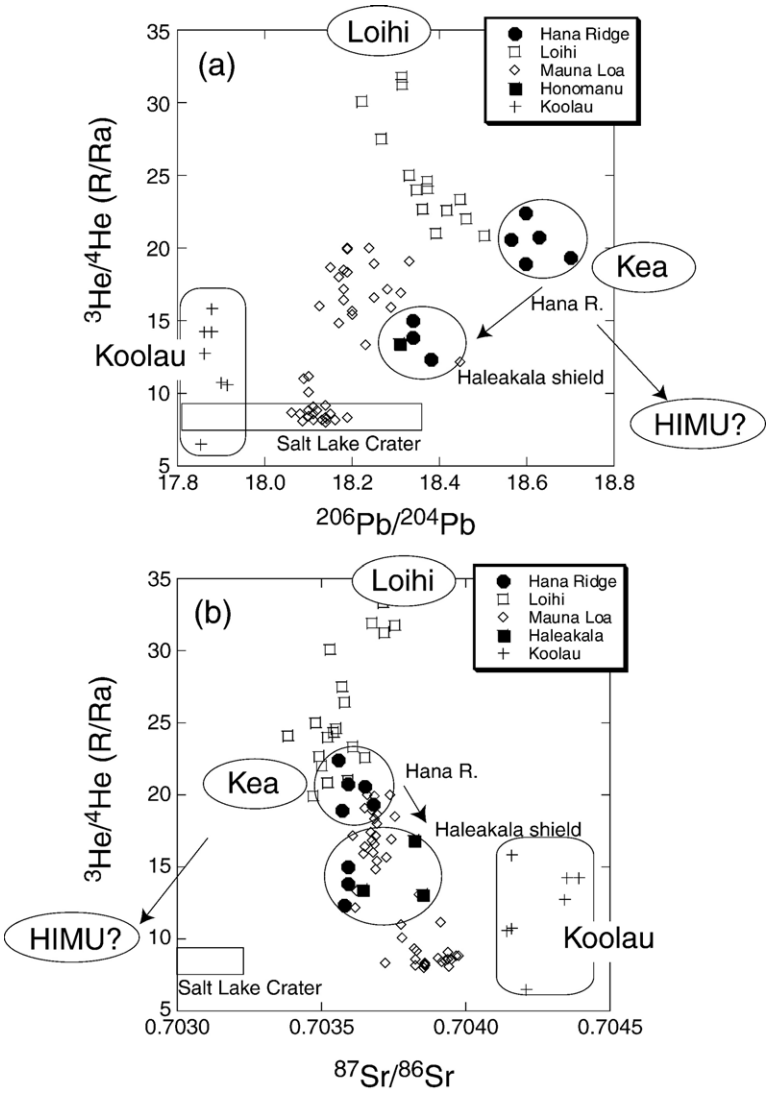

Fig. 6. Relationships between $^{3}He/^{4}He$ and (a) $^{206}Pb/^{204}Pb$ and (b) $^{87}Sr/^{86}Sr$ among the Hawaiian lavas. Assumed endmember components are shown as "Loihi", "Kea" and "Koolau". Another possible endmember in the Hawaiian plume would be the depleted lithosphere and asthenosphere represented by Salt Lake Crater xenoliths. The data sources for Loihi, Mauna Loa, Haleakala shield (Honomanu) and Koolau are Kurz et al. (1983), Rison and Craig (1983), Staudigel et al. (1984), Chen et al. (1991), Kurz and Kammer (1991), Honda et al. (1993a), Kurz et al. (1987), Roden et al. (1994), Kurz et al. (1995), Cohen et al. (1996), Valbracht et al. (1996), Garcia et al. (1998), Lassiter and Hauri (1998) and Roy-Barman et al. (1998). Salt Lake Crater xenoliths data are from Okano and Tatsumoto (1996).

and "Kea" (Fig. 6). Most of the Hana Ridge samples have relatively high $^{206}Pb/^{204}Pb$ among the Hawaiian samples and plot on the extension of the trend defined by Loihi samples. The source of the Hana Ridge samples therefore involves the "Kea" component more so than the source of Loihi magmas. The general existence of "Kea" component in the Hawaiian mantle plume is also demonstrated by Pb–Sr–Nd–Hf isotopic evidence that most of the shield building tholeiitic rocks define a single trend in isotope diagrams between "Kea" and "Koolau" (Blichert-Toft et al., 1999). Consequently, the "Kea" component is the major component both for pre-shield stage Loihi lavas and the shield stage tholeiites. As Hana Ridge samples have isotopic compositions close to the "Kea" component, these samples can be representative of the "Kea" component, and the present noble gas data suggest that the "Kea" component should have lower $^{3}He/^{4}He$ than the "Loihi" component, but higher $^{3}He/^{4}He$ than MORB (Fig. 6).

Some previous studies have proposed that the Kea component was derived from 'young' (<1.5 Ga) recycled oceanic crust (Eisele et al., 2003), or derived

from young HIMU (high-μ) mantle (Thirlwall, 1997). However, melting experiments (Kogiso et al., 1998; Takahashi and Nakajima, 2002) show that picritic primary magma of Kea lavas (e.g., 16–17 wt.% MgO; Chen, 1993; Clague et al., 1995; Wagner et al., 1998; Ren et al., 2004) could not be derived from melting of recycled oceanic basaltic composition. Furthermore, this model requires explanation for the moderately high $^{3}He/^{4}He$ values in Kea lavas, because if the "Kea" component is recycled oceanic crust, it would have a very low $^{3}He/^{4}He$ value due to degassing of He and subsequent radiogenic ingrowth of ^{4}He. Lassiter and Hauri (1998) postulated that the "Kea" component was derived from recycled, hydrothermally altered, ultramafic lower crust or lithospheric mantle as Kea lavas have unradiogenic Os isotopes and anomalously light oxygen isotopes. However, this model is also insufficient to explain high $^{3}He/^{4}He$ ratios in Kea lavas.

We would propose that the "Kea" component is not a distinct pure endmember but a sub-component that is a mixture of the "Loihi" and another component having isotopic characteristics plotting on the extension of the trend defined by Loihi and Hana Ridge samples (Fig. 6). This component should have even higher $^{206}Pb/^{204}Pb$ and lower $^{87}Sr/^{86}Sr$ in comparison to those ratios of Hana Ridge samples. These isotopic characteristics are probably similar to a HIMU endmember; recycled oceanic crust. As HIMU have relatively low $^{3}He/^{4}He$ due to increased (U+Th)/He ratio and long-term isolation, mixing of HIMU endmember and "Loihi" endmember should result in moderately high $^{3}He/^{4}He$ associated with relatively high $^{206}Pb/^{204}Pb$ and low $^{87}Sr/^{86}Sr$ ratios of the "Kea" sub-component (Fig. 6).

Our new preferred model explains why the "Kea" sub-component is a common component existing in the Hawaiian mantle plume. We believe that the Hawaiian plume comprises peridotite from a primordial reservoir ("Loihi") and eclogite from recycled oceanic crust (HIMU). Eclogite fuses first at great depth in the peridotitic matrix in the ascending mantle plume (Yasuda et al., 1994; Yaxley and Green, 1998). The melt would react with peridotite to produce pyroxenite (Yasuda et al., 1994; Yaxley and Green, 1998; Takahashi and Nakajima, 2002; Sobolev et al., 2005). This secondary pyroxenite would have isotopic compositions intermediate between "Loihi" and "HIMU", geochemically characterizing the "Kea" sub-component (Fig. 6). Then, the mantle plume, including the unreacted peridotite and secondary pyroxenite that are distributed heterogeneously, undergo major melting at shallow depth. Since the temperature is relatively high at the center of the mantle plume, both the unreacted peridotite ("Loihi") and the secondary pyroxenite ("Kea") melt at the beginning of the volcanic growth. The melts produced in this stage would have compositions intermediate between the two, thus the Loihi Seamount samples plot along the mixing lines between "Loihi" and "Kea" in the He–Pb–Sr diagrams (Fig. 6). In the periphery of the plume, where temperature is relatively low, melts derived from secondary pyroxenite dominates melts from peridotite, and the "Kea" signature is the major expression during the shield stage.

4.3. Involvement of enriched component in the later stage magma of Haleakala

The submarine Hana Ridge and the subaerial Honomanu tholeiites consist of two groups with distinct $^{3}He/^{4}He$ ratios that are correlated with Pb–Sr isotope ratios (Fig. 6). Several models have been proposed for lowering the $^{3}He/^{4}He$ ratios during the shield stage, such as (1) crustal contamination (Kaneoka et al., 2002), (2) degassing and in-situ ^{4}He ingrowth (Kurz et al., 1983), (3) reduction of plume flux and contribution of the ambient depleted mantle (Valbracht et al., 1996; DePaolo et al., 2001), (4) incorporation of recycled components (Kaneoka et al., 2002; Althaus et al., 2003).

The post-shield and rejuvenated stage magmas as well as submarine alkalic basalts distributed widely around the Hawaiian shield volcanoes show comparable $^{3}He/^{4}He$ ratios as MORBs, which is best explained by melting of the depleted mantle with little plume flux (Kurz et al., 1987; Vance et al., 1989; Hanyu et al., 2005). Pb–Sr–Nd isotope data are in accordance with this model, as those magmas show more depleted isotopic characteristics than the shield stage magmas. However, the $^{3}He/^{4}He$ variation of Haleakala shield, including the submarine Hana Ridge and subaerial Honomamu lavas, cannot be accounted for by simple mixing of the less-degassed component and the depleted mantle (Fig. 6). Ren et al. (2006) have demonstrated that most of submarine Hana Ridge samples have lower $^{87}Sr/^{86}Sr$ and higher $^{143}Nd/^{144}Nd$ ratios than Honomamu lavas. Therefore, the Hana Ridge magmas should have involved a more depleted component than the Honomanu magmas. This contradicts the observation that Honomanu lavas have lower $^{3}He/^{4}He$ ratios than Hana Ridge lavas, and suggests that simple mixing of a less-degassed component and depleted mantle can be ruled out to reduce $^{3}He/^{4}He$ during the shield stage of Haleakala volcano.

Crustal contamination or degassing and subsequent in-situ ^{4}He ingrowth is unlikely because $^{3}He/^{4}He$ ratios are relatively constant irrespective of ^{4}He concentrations among most of the Hana Ridge samples.

Furthermore, coupled behavior of He and Pb–Sr isotopes may not be explained by such processes.

Among the Hawaiian volcanoes, Koolau shows the most enriched and EM-1 like isotopic signatures. Hauri (1996) and Lassiter and Hauri (1998) asserted that the Koolau source involves a significant amount of recycled oceanic crust plus pelagic sediment. Emplacement of the lavas with strong "Koolau" signature is, however, limited at the upper part of the Koolau volcano, and the lower portion of the Koolau shield lavas have relatively depleted Sr and Nd isotope signatures (Jackson et al., 1999; Tanaka and Nakamura, 2002). This may be explained as melt from recycled material in the mantle plume being trapped in the magma source in the late stage of the volcanic growth. This scenario was further supported by He isotopic signatures in samples collected from the submarine flank of the Koolau (Kaneoka et al., 2002). The samples collected at the shallower part (less than 3000 m depth) have $^{3}He/^{4}He$ between 14 and 15 Ra that overlap with the ratios of subaerial Koolau lavas (Roden et al., 1994). In contrast, the lavas from the deep portion of the shield show relatively high $^{3}He/^{4}He$ (19 Ra). This Koolau model can account for the He and Pb–Sr–Nd isotopic variations among the lavas from Haleakala as well. Provided EM-1 was a recycled component, it should have low $^{3}He/^{4}He$ ratios. Incorporation of such a component in the source magmas that produced original Hana Ridge lavas (mostly equivalent to "Kea") will reduce $^{3}He/^{4}He$ and change Sr–Nd–Pb isotopic features toward a Koolau endmember, which produced Honomamu lavas.

4.4. Implication for the formation of the Hana Ridge

The studied samples were collected from diverse places and depths from the ridge. Most of the samples have He–Pb–Sr isotopic compositions close to the "Kea" component. Constancy of these isotopic compositions for such samples suggests that the eastern half of the Hana Ridge had been formed by magmas with uniform compositions. $^{40}Ar/^{39}Ar$ ages ranging from 1.3–1.9 Ma suggest that Hana Ridge was built over a period of at least 0.6 My by lavas derived from a relatively uniform magma source. It has been recognized that there are at least three structural lineaments that branch from the central part of the ridge. It was previously suggested that these lineaments probably reflect the evolution of the ridge system as the relative position of the ridge from the plume center shifts (Smith et al., 2002). The present age data do not show systematic age difference or geochemical compositions between the lineaments, supporting a model of contemporaneous, not sequential, growth of the three ridge lineaments.

We interpret the prevalence of younger ages among our samples to represent resurfacing during growth of the ridge. Three exposures of 1.8 and 1.9 Ma lavas and two intermediate-aged lavas represent older growth stages. Subaerial Haleakala shield lavas of the Honomanu Series were dated at 1.1–0.97 Ma (Chen et al., 1991). Thus, it appears that the lower Hana Ridge grew over a period of 0.6 My and that shield building on Haleakala continued for nearly 1 My. This is considerably longer than some estimates of the duration of tholeiitic volcanism (Wright et al., 1979; Lipman et al., 2002) and similar to other estimates (Jackson et al., 1972; Clague and Dalrymple, 1987; Guillou et al., 1997). Our directly measured ages put firm constraints on the duration of shield growth at Haleakala volcano.

In two locations (K212 and K216), shallowest sampled lavas were older than deeper-sampled lavas. Very fresh, glassy, young lava flows have also been observed on the flanks of the Puna Ridge, below more weathered, presumably older flows (Johnson et al., 2002; Smith et al., 2002). We infer from this observation that growth of these ridges takes place endogenously by continuous intrusion of magma along the rift zone (Francis et al., 1993). Resurfacing of the ridge occurs when intrusions erupt, but some lavas exposed at shallower water depth may be older than lavas found at deeper water depths.

The three samples from the K214 site, K214-9, K214-15A and K214-15D, have exceptionally low $^{3}He/^{4}He$ among the Hana Ridge samples. It is likely that K214-15A and K214-15D were later stage rocks similar to the subaerial Honomamu tholeiites that may have fallen down the slope. K214-9, however, was a pillow lava collected from an outcrop. One possibility is that K214-9 sample was a late intrusion of lavas into the ridge, although the age of a nearby sample is 1.4 Ma, the same as the majority of Hana Ridge lavas. Another possibility is that magma that involves melt from a recycled blob (EM-1) was occasionally fed to the shallow magma chamber and erupted to the submarine ridge. Short time scale excursion of the high $^{3}He/^{4}He$ is reported for the Mauna Kea shield lavas by Hawaiian Scientific Drilling Project (Kurz et al., 2004). The Hana Ridge magmas may demonstrate the opposite trend of excursion to Mauna Kea; low $^{3}He/^{4}He$ pulses among dominantly high $^{3}He/^{4}He$ magmas.

4.5. He–Ne–Ar systematics of the Hawaiian plume source

Ne isotope ratios, as well as He isotope ratios, have great potential to resolve the less degassed component in

the magma source. The Hana Ridge samples define a clear correlation trend that is equivalent to the Loihi–Kilauea trend in the Ne-three-isotope diagram. This is consistent with the magma source that established the Hana Ridge involving the less-degassed component. However, decoupling between He and Ne isotopes is highlighted by the present data. It has been recognized that Loihi with $^{3}He/^{4}He$ greater than 25 Ra and Kilauea with $^{3}He/^{4}He$ of around 14 Ra reproduce a similar $^{20}Ne/^{22}Ne$ – $^{21}Ne/^{22}Ne$ trend. Althaus et al. (2003) demonstrated similar decoupled behavior between He and Ne isotopes for samples from the HSDP site. The apparent decoupling between $^{4}He/^{3}He$ and $(^{21}Ne/^{22}Ne)_m$ is clearly illustrated in Fig. 7 where $(^{21}Ne/^{22}Ne)_m$ is an atmosphere-free ratio (definition is shown in the caption of Fig. 7). Our data indicate that the lavas associated with moderately high $^{3}He/^{4}He$ (low $^{4}He/^{3}He$) show similar $(^{21}Ne/^{22}Ne)_m$ values to Loihi, Kilauea and Mauna Kea, and confirm little variation of $(^{21}Ne/^{22}Ne)_m$ irrespective of $^{3}He/^{4}He$ ratios among Hawaiian magmas.

It has been recognized that OIBs and MORBs define a concave trend in the $^{4}He/^{3}He$–$(^{21}Ne/^{22}Ne)_m$ diagram.

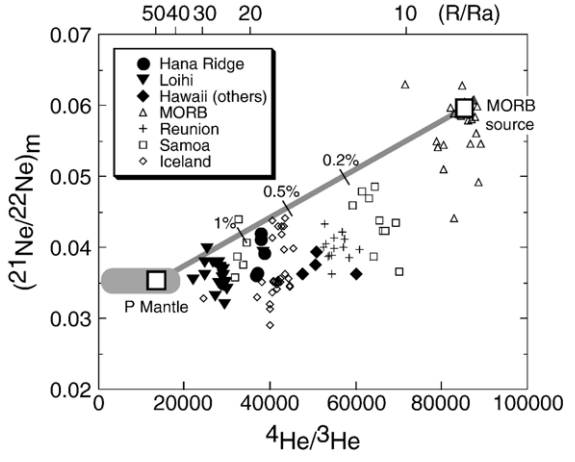

Fig. 7. $(^{21}Ne/^{22}Ne)_m$ versus $^{4}He/^{3}He$ for the Hawaiian samples and other OIBs and MORBs. $(^{21}Ne/^{22}Ne)_m$ denotes the atmosphere free $^{21}Ne/^{22}Ne$ ratio which can be calculated by extrapolating the Ne data point from atmospheric value to the plume endmember at $^{20}Ne/^{22}Ne$ value of 12.5. The mixing calculation between primordial mantle (P-Mantle) and MORB source is carried out by assuming the endmember isotopic composition and elemental abundances from Porcelli and Wasserburg (1995). The Hana Ridge data with other Hawaiian data define a near-horizontal trend in the diagram, suggesting local mixing processes alter He isotope ratios drastically in comparison with the relatively constant and primordial Ne isotopes. The data sources for other hotspots and MORBs are Sarda et al. (1988), Honda et al. (1991), Hiyagon et al. (1992), Poreda and Farley (1992), Honda et al. (1993b), Valbracht et al. (1997), Harrison et al. (1999), Trieloff et al. (2000), Dixon et al. (2000), Hanyu et al. (2001), Moreira et al. (2001), Trieloff et al. (2002) and Althaus et al. (2003).

The trend consists of two parts. The left half of the trend is defined by OIBs having constant $(^{21}Ne/^{22}Ne)_m$ and relatively low $^{4}He/^{3}He$. MORBs show relatively high $^{4}He/^{3}He$ and variable $(^{21}Ne/^{22}Ne)_m$, establishing the upper-right half of the trend. Hawaiian data, including the Hana Ridge, overlap nearly the entire range established by OIB data. The cause of the trend established by the Hawaiian data may be different from that of the global trend, but is attributed to a local mixing effect as demonstrated by correlated He–Pb–Sr isotopes. Here, we focus on discussing the process responsible for producing a near-horizontal trend among Hawaiian samples in the $^{4}He/^{3}He$–$(^{21}Ne/^{22}Ne)_m$ diagram (Fig. 7).

Variation of $^{3}He/^{4}He$ coupled with Pb–Sr isotopes between Loihi, Kilauea and Hana Ridge is best explained by mixing of "Loihi" and "Kea" components, the latter of which is a product of reaction between a peridotitic "Loihi" component and recycled oceanic crust, as proposed above. The apparent decoupling between He and Ne isotopes thus requires that reaction of the recycled oceanic crust with peridotite should not alter primordial Ne isotope characteristics. A possible explanation is that Ne concentration of the recycled crust was much smaller than that of "Loihi" while contribution of He from both components was relatively comparable. This possibility was assessed to account for the He–Ne systematics of Afar plume rocks that were produced by mixing of mantle plume and subcontinental lithospheric mantle (SCLM) (Hopp et al., 2004). They supposed that SCLM had greater $^{4}He/^{3}He$ and $(^{21}Ne/^{22}Ne)_m$ than the MORB source due to radiogenic/nucleogenic ingrowth in a closed system, and recent degassing for SCLM caused lowering of Ne/He. The recycled oceanic crust would also possess elevated $^{4}He/^{3}He$ and $(^{21}Ne/^{22}Ne)_m$, although fractionation processes to alter Ne/He are still unconstrained. An alternative model is that fractionation occurred within the plume to increase the Ne/He ratio of the "Loihi" component. DePaolo et al. (2001) and Hanyu et al. (2005) proposed that melting took place incrementally, producing volatile rich melt at the beginning, followed by volatile-poor melt production from the residue that underwent prior melt extraction. The later melt should have greater Ne/He than the early melt if He is more incompatible than Ne during partial melting (e.g., Broadhurst et al., 1992), although incompatibility between the two elements may not be different enough to fractionate Ne/He ratios in the residues (Brooker et al., 2003). Alternative process might be a kinetic loss of He during degassing of the plume source. If a plume melt produced from rocks after incremental melt extraction mixes with melt from recycled material, Ne/He of the

plume melt would be greater than that of recycled material.

5. Conclusions

The $^{40}Ar/^{39}Ar$ ages demonstrate that the Hana Ridge was emplaced between 1.3–1.9 Ma and that it predates the Honomamu Series on the shield volcano of Haleakala (1.1–0.97 Ma). The ages indicate that the submarine rift zones have recorded early stage magmatic activity that is rarely obtained on shield volcanoes due to blanketing by late stage lavas. The presence of a few samples with ages up to 1.9 Ma suggest that intrusion of magmas along the rift zone that built Hana Ridge persisted over a period of at least 0.5 My, and that whole activity of tholeiitic magmatism at Haleakala continued over a period of 1 My.

Most samples from Hana Ridge have uniform isotopic compositions that resemble the "Kea" component. Elevated $^{3}He/^{4}He$ ratios coupled with high $^{206}Pb/^{204}Pb$ and low $^{87}Sr/^{86}Sr$ ratios that characterize this component is best explained by mixing of less-degassed "Loihi" component and recycled oceanic crust. We interpret the "Kea" component as being produced by reaction of peridotite from less-degassed mantle ("Loihi") with partial melts of the recycled oceanic crust distributed in the mantle plume. This reaction took place at a great depth prior to major melting in the upwelling mantle plume, and formed pyroxenite with "Kea" isotopic characteristics. In contrast, Honomanu tholeiites and three samples from the Hana Ridge show low $^{3}He/^{4}He$, low $^{206}Pb/^{204}Pb$ and high $^{87}Sr/^{86}Sr$ in comparison to the majority of the Hana Ridge samples. This is best explained by involvement of an EM-1-like component, equivalent to the "Koolau" component.

Ne isotope ratios of the Hawaiian lavas, including Hana Ridge, demonstrate equally primordial characteristics irrespective of $^{3}He/^{4}He$ ratios. Although the trend between $^{4}He/^{3}He$ and $(^{21}Ne/^{22}Ne)_m$ among the Hawaiian samples apparently overlap the global trend defined by OIBs and MORBs, the former trend is attributed to a local mixing process. Addition of the recycled component to "Loihi" did not alter the primordial Ne isotopic signature, despite reduction of $^{3}He/^{4}He$, presumably due to Ne/He fractionation in either component prior to mixing.

Acknowledgements

We thank the scientific party, the crews on the R/V Yokosuka and Kairei and the operation teams of submersibles Shinkai 6500 and Kaiko of JAMSTEC Hawaiian research cruises in 2001–2002. T. H. is grateful to H. Kumagai, K. Sato and J. Tamura for their help to establish a noble gas laboratory at JAMSTEC. H. Hyodo, T. Itaya, I. Kaneoka and Y. Miura are acknowledged for providing standard helium gas samples to T. H. Eight of the $^{40}Ar/^{39}Ar$ analyses reported in this paper were carried out at the Oregon Stage University Geochronology Lab, and we thank J. Huard and R. Duncan for their helpful discussions related to this work. We are also grateful to the staff of the International Research Center for Nuclear Materials Science, Institute for Materials Research, Tohoku University and the staff of Japan Material Testing Reactor of the Japan Atomic Energy Research Institute for the neutron irradiation of two additional samples for $^{40}Ar/^{39}Ar$ dating. We would like to thank K. Nagao, Y. Takigami, M. Morioka and H. Sumino for $^{40}Ar/^{39}Ar$ dating analyses of these samples at Radioisotope Center, University of Tokyo. Thanks are also due to Y. Tatsumi for his support and encouragement on this study. This work was supported by NSF-0408270 and this is SOEST contribution 6911 (K. T. M. J.).

Appendix A. Experimental methods

A.1. Noble gases

Rock samples were crushed by a jaw crusher and olivine phenocrysts were handpicked under binocular. The typical grain size of olivine was 0.5–1.5 mm. They were leached in warm (70 °C) 5% nitric acid to remove surface contaminants, then washed ultrasonically by acetone, ethanol and distilled water.

Gas extraction was carried out by either crushing or heating in vacuum. The crusher consists of a metal tube and a piston that is lifted by a solenoid coil and released repeatedly. After loading the samples in the crushing tube, they were baked over night at 150–200 °C in vacuum. Most of the samples were crushed by a single step of 100 strokes. Stepwise crushing was carried out for some selected samples to assess the crushing efficiency and the possible influence of post-eruptive radiogenic component. For the heating experiments, samples were loaded in a glass sample holder and baked out at 180 °C for two days. A molybdenum crucible was degassed at 1900–2000 °C to reduce the hot blank prior to each sample run, then samples were dropped into the crucible. A two-stepwise heating scheme at 800 °C and 1850 °C was applied for gas extraction.

Gases extracted either by crushing or heating were purified using three titanium–zirconium hot getters and a cold SAES getter to remove active gases. Helium,

neon and argon were separated by activated charcoal cooled by liquid nitrogen and sintered stainless cooled by cryogenic pump at 20 K. For some selected samples, xenon was separated from argon using activated charcoal at −20 °C for xenon isotopic analysis.

Measurement of noble gas abundances and isotope ratios were performed on a sector-type mass spectrometer (GVI-5400) at JAMSTEC. He isotope ratios were normalized by repeated measurements of the standard gas from Kaminoyama well (5.68 Ra), $^{3}He/^{4}He$ of which had been cross-calibrated by atmospheric helium (1 Ra) and HESJ (He standard of Japan; 20.63 Ra) (Matsuda et al., 2002). The other isotope ratios and noble gas abundances were calibrated by repeated measurements of diluted air. Typical blank levels by crushing and heating are shown in Tables 2 and 3, respectively. All the reported data were blank corrected. Neon isotope ratios were corrected for interferences of $^{40}Ar^{+}$ and CO_2^{+} on $^{20}Ne^{+}$and $^{22}Ne^{+}$, respectively.

A.2. $^{40}Ar/^{39}Ar$ analyses

Eight samples, K212-4, K212-13B, K214-7, K214-10, K216-3, K216-10, S687-5 and S691-2A, were selected for dating by the $^{40}Ar/^{39}Ar$ method at Oregon State University based on location, lack of alteration, and aphyric texture. In some cases, phenocrysts were present, but were avoided as much as possible when preparing the sample for analysis.

Samples were prepared using either of two methods depending on mineralogy, texture and evidence of alteration. Aphyric rocks were prepared by drilling minicores (5 mm diameter) from the freshest interiors of sawn surfaces. These minicores were then sliced into approximately 300 mg disks using a diamond-impregnated fine bandsaw, and marked for identification. The vesicular or olivine phenocryst bearing samples were crushed, sieved and groundmass separated using a Franz isodynamic separator. Groundmass separates were treated with a mild acid leaching procedure to remove small amounts of clay or carbonates. This consisted of an ultrasonic wash in diluted nitric acid for 20 min, distilled water rinse, and then drying. Groundmass separates were then examined with a binocular microscope and remaining olivine crystals removed by hand. Approximately 200 mg of the final groundmass separates were wrapped in Cu-foil and marked for identification.

Samples, both whole rock disks and Cu-wrapped groundmass separates, were stacked in quartz vials which were evacuated and sealed. Quartz vials were then placed in an aluminum TRIGA irradiation tube. Samples were irradiated at Oregon State University TRIGA research reactor for 6 hors at 1 MW power and the neutron fluence monitored with Fish Canyon Tuff biotite standard (28.03 ± 0.16 Ma; Renne et al., 1998), spaced at regular intervals among the sample unknowns. Errors in monitor measurements and gradient fitting accumulated to about 0.5%.

Following irradiation and the initial decay of short-lived radionuclides, samples were loaded into an ultra-high vacuum gas extraction line. A double-vacuum resistance furnace with thermocouple-controlled temperature and a Ta-crucible (internal Mo-sleeve) was used for sample gas extraction. Samples were heated incrementally from 400 °C to 1400 °C in 100 °C to 200 °C steps depending on K-content. The extracted gas per heating increment was cleaned to remove active gases using Zr–Al and Zr–Fe–Al getters, then isotopic compositions of Ar released were determined with a MAP 215/50 noble gas mass spectrometer.

The Ar data were acquired in a peak-jumping mode (for m/z=35, 36, 37, 38, 39, 40). Peak decay was typically linear and <10% over 10 sets of each mass peak and baseline. Mass discrimination on the MAP system was measured with zero age samples run in the same way as samples, and was constant at 1.005 (for 2 amu). The sensitivity of the mass spectrometer is 4×10^{-14} mol/V and measured backgrounds were 1.5×10^{-18} mol at m/z=36, 2×10^{-18} mol at m/z=39 and 1.5×10^{-16} mol at m/z=40. Procedural blanks for the resistance furnace ranged from 3.0×10^{-18} mol ^{36}Ar and 9.0×10^{-16} mol ^{40}Ar at 600 °C to 6.4×10^{-18} mol ^{36}Ar and 1.9×10^{-15} mol ^{40}Ar at 1400 °C (Duncan, 2001).

Further $^{40}Ar/^{39}Ar$ dating was conducted for two samples, K212-3A and S686-2A, at University of Tokyo. The sample preparation procedure was principally similar to the way described above. Samples were wrapped in aluminum foil, then placed in an aluminum tube (70 mm in length, 10 mm in diameter) with flux monitors of EB-1 biotite (91.4±0.5 Ma; Iwata, 1998), K_2SO_4 and CaF_2. The samples were irradiated for 24 h in the Japan Material Testing Reactor (JMTR), Tohoku University. During the irradiation, the samples were shielded by Cd-foil in order to reduce thermal neutron-induced ^{40}Ar from ^{40}K. The Ar extraction and Ar isotopic analyses were conducted at Radioisotope Center, University of Tokyo. During incremental heating, gases were extracted in each of 9 steps between 600 and 1500 °C. After purification of extracted gases by Ti–Zr getters, Ar isotope ratios and abundances were determined with a VG3600 noble gas mass spectrometer by a peak-jumping mode. The detailed analytical methods and typical blanks are described elsewhere (Ebisawa et al., 2004).

References

Abouchami, W., Hofmann, A.W., Galer, S.J.G., Frey, F.A., Eisele, J., Feigenson, M., 2005. Lead isotopes reveal bilateral asymmetry and vertical continuity in the Hawaiian mantle plume. Nature 434, 851–856.

Althaus, T., Niedermann, S., Erzinger, J., 2003. Noble gases in olivine phenocrysts from drill core samples of the Hawaii Scientific Drilling Project (HSDP) pilot and main holes (Mauna Loa and Mauna Kea, Hawaii). Geochem. Geophys. Geosyst. 4. doi:10.1029/2001GC000275.

Blichert-Toft, J., Frey, F.A., Albarède, F., 1999. Hf isotope evidence for pelagic sediments in the source of Hawaiian basalts. Science 285, 879–882.

Blichert-Toft, J., Weis, D., Maerschalk, C., Agranier, A., Albarède, F., 2003. Hawaiian hot spot dynamics as inferred from the Hf and Pb isotope evolution of Mauna Kea volcano. Geochem. Geophys. Geosyst. 4. doi:10.1029/2002GC000340.

Broadhurst, C.L., Drake, M.J., Hagee, B.E., Bernatowicz, T.J., 1992. Solubility and partition of Ne, Ar, Kr, and Xe in mineral and synthetic basalt melts. Geochim. Cosmochim. Acta 56, 709–723.

Brooker, R.A., Du, Z., Blundy, J.D., Kelley, S.P., Allan, N.L., Wood, B.J., Chamorro, E.M., Wartho, J.-A., Purton, J.A., 2003. The 'zero charge' partitioning behaviour of noble gases during mantle melting. Nature 423, 738–741.

Bryce, J.G., DePaolo, D.J., Lassiter, J.C., 2005. Geochemical structure of the Hawaiian plume: Sr, Nd, and Os isotopes in the 2.8 km HSDP-2 section of Mauna Kea volcano. Geochem. Geophys. Geosyst. 6. doi:10.1029/2004GC000809.

Chen, C.-Y., 1993. High-magnesium primary magmas from Haleakala volcano, east Maui, Hawaii: petrography, nichel, and major-element constraints. J. Volcanol. Geotherm. Res. 55, 143–153.

Chen, C.-Y., Frey, F.A., 1985. Trace element and isotopic geochemistry of lavas from Haleakala volcano, East Maui: implications for the origin of Hawaiian basalts. J. Geophys. Res. 90, 8743–8768.

Chen, C.-Y., Frey, F.A., Garcia, M.O., Dalrymple, G.B., Hart, S.R., 1991. The tholeiite to alkalic basalt transition at Haleakala Volcano, Maui, Hawaii. Contrib. Mineral. Petrol. 106, 183–200.

Clague, D.A., Dalrymple, G.B., 1987. The Hawaiian-Emperor volcanic chain, part 1, Geologic evolution. U. S. Geol. Surv. Prof. Pap. 1350, 5–54.

Clague, D.A., Moore, J.G., Dixon, J.E., Friesen, W.B., 1995. Petrology of submarine lavas from Kilauea's Puna Ridge, Hawaii. J. Petrol. 36, 299–349.

Clague, D.A., Moore, J.G., Reynolds, J.R., 2000. Formation of submarine flat-topped volcanic cones in Hawai'i. Bull. Volcanol. 62, 214–233.

Cohen, A.S., O'Nions, R.K., Kurz, M.D., 1996. Chemical and isotopic variations in Mauna Loa tholeiites. Earth Planet. Sci. Lett. 143, 111–124.

Courtillot, V., Davaille, A., Besse, J., Stock, J., 2003. Three distinct types of hotspots in the Earth's mantle. Earth Planet. Sci. Lett. 205, 295–308.

Davies, G.F., 1988. Ocean bathymetry and mantle convection, 1, Large-scale flow and hotspots. J. Geophys. Res. 93, 10467–10480.

DePaolo, D.J., Bryce, J.G., Dodson, A., Shuster, D.L., Kennedy, B.M., 2001. Isotopic evolution of Mauna Loa and the chemical structure of the Hawaiian plume. Geochem. Geophys. Geosyst. 2. doi:10.1029/2000GC000139.

Dixon, E.T., Honda, M., McDougall, I., Campbell, I.H., Sigurdsson, I., 2000. Preservation of near-solar neon isotopic ratios in Icelandic basalts. Earth Planet. Sci. Lett. 180, 309–324.

Duncan, R.A., 2001. A time frame for construction of the Kerguelen Plateau and Broken Ridge. J. Petrol. 43, 1109–1119.

Eakins, B.W., Robinson, J.E., 2006. Submarine geology of Hana Ridge and Haleakala Volcano's northeast flank, Maui. J. Volcanol. Geotherm. Res. 151, 229–250.

Ebisawa, N., Sumino, H., Okazaki, R., Takigami, Y., Hirano, N., Nagao, K., Kaneoka, I., 2004. Construction of I–Xe and 40Ar–39Ar dating system using a modified VG3600 noble gas mass spectrometer. J. Mass Spectrom. Soc. Jpn. 52, 219–229.

Eiler, J.M., Farley, K.A., Valley, J.W., Hofmann, A.W., Stolper, E.M., 1996. Oxygen isotope constraints on the sources of Hawaiian volcanism. Earth Planet. Sci. Lett. 144, 453–468.

Eisele, J., Abouchami, W., Galer, S.J.G., Hofmann, A.W., 2003. The 320 kyr Pb isotope evolution of Mauna Kea lavas recorded in the HSDP-s drill core. Geochem. Geophys. Geosyst. 4. doi:10.1029/2002GC000339.

Francis, P., Oppenheimer, C., Stevenson, D., 1993. Endogenous growth of persistently active volcanoes. Nature 366, 554–557.

Frey, F.A., Rhodes, J.M., 1993. Intershield geochemical differences among Hawaiian volcanoes: implications for source compositions, melting processes and magma ascent paths. Philos. Trans. R. Soc. Lond. Ser. A: Math. Phys. Sci. 352, 121–136.

Garcia, M.O., Rubin, K.H., Norman, M.D., Rhodes, J.M., Graham, D.W., Muenow, D.W., J., S.K., 1998. Petrology and geochronology of basalt breccia from the 1996 earthquake swarm of Loihi Seamount, Hawaii; magmatic history of its 1996 eruption. Bull. Volcanol. 59, 577–592.

Guillou, H., Turpin, L., Garnier, F., Charbit, S., Thomas, D.M., 1997. Unspiked K–Ar dating of Pleistocene tholeiitic basalts from the deep core SOH-4, Kilauea, Hawaii. Chem. Geol. 140, 81–88.

Hanyu, T., Dunai, T.J., Davies, G.R., Kaneoka, I., Nohda, S., Uto, K., 2001. Noble gas study of the Reunion hotspot: evidence for distinct less-degassed mantle sources. Earth Planet. Sci. Lett. 193, 83–98.

Hanyu, T., Clague, D.A., Kaneoka, I., Dunai, T.J., Davies, G.R., 2005. Noble gas systematics of sumarine alkalic lavas near the Hawaiian hotspot. Chem. Geol. 214, 135–155.

Harrison, D., Burnard, P., Turner, G., 1999. Noble gas behaviour and composition in the mantle: constraints from the Iceland Plume. Earth Planet. Sci. Lett. 171, 199–207.

Hauri, E.H., 1996. Major-element variability in the Hawaiian mantle plume. Nature 382, 415–419.

Hauri, E.H., Lassiter, J.C., DePaolo, D.J., 1996. Osmium isotope systematics of drilled lavas from Mauna Loa, Hawaii. J. Geophys. Res. 101, 11793–11806.

Hiyagon, H., Ozima, M., Marty, B., Zashu, S., Sakai, H., 1992. Noble gases in submarine glasses from mid-oceanic ridges and Loihi seamount: constraints on the early history of the Earth. Geochim. Cosmochim. Acta 56, 1301–1316.

Honda, M., McDougall, I., Patterson, D.B., Doulgeris, A., Clague, D.A., 1991. Possible solar noble-gas component in Hawaiian basalts. Nature 349, 149–151.

Honda, M., McDougall, I., Patterson, D., 1993a. Solar noble gases in the Earth: the systematics of helium–neon isotopes in mantle derived samples. Lithos 30, 257–265.

Honda, M., McDougall, I., Patterson, D.B., Doulgeris, A., Clague, D.A., 1993b. Noble gases in submarine pillow basalt glasses from Loihi and Kilauea, Hawaii: a solar component in the Earth. Geochim. Cosmochim. Acta 57, 859–874.

Hopp, J., Trieloff, M., Altherr, R., 2004. Neon isotopes in mantle rocks from the Red Sea region reveal large-scale plume–lithosphere interaction. Earth Planet. Sci. Lett. 219, 61–76.

Iwata, N., 1998. Geochronological study of the Decan volcanism by the ^{40}Ar–^{39}Ar method. Ph. D. thesis, University of Tokyo.

Jackson, E.D., Silver, E.A., Dalrymple, G.B., 1972. Hawaiian-Emperor Chain and its relation to Cenozoic circum-Pacific tectonics. Geol. Soc. Amer. Bull. 83, 601–618.

Jackson, M.C., Frey, F.A., Garcia, M.O., Wilmoth, R.A., 1999. Geology and geochemistry of basaltic lava flows and dikes from the Trans-Koolau tunnel, Oahu, Hawaii. Bull. Volcanol. 60, 381–401.

Johnson, K.T.M., Reynolds, J.R., Smith, D.K., Kong, L.S.L., Vonderhaar, D., 2002. Petrological systematics of submarine basalt glasses from the Puna Ridge, Hawai'i: implications for rift zone plumbing and matmatic processes. In: Takahashi, E., Lipman, P.W., Garcia, M.O., Naka, J., Aramaki, S. (Eds.), Hawaiian Volcanoes, Deep Underwater Perspectives. Geophysical Monograph, vol. 128, pp. 143–160.

Kaneoka, I., Takaoka, N., Clague, D.A., 1983. Noble gas systematics for coexisting glass and olivine crystals in basalts and dunite xenoliths from Loihi Seamount. Earth Planet. Sci. Lett. 66, 427–437.

Kaneoka, I., Hanyu, T., Yamamoto, J., Miura, Y.N., 2002. Noble gas systematics of the Hawaiian volcanoes based on the analysis of Loihi, Kilauea and Koolau submarine rocks. In: Takahashi, E., Lipman, P.W., Garcia, M.O., Naka, J., Aramaki, S. (Eds.), Hawaiian Volcanoes, Deep Underwater Perspectives. Geophysical Monograph, vol. 128, pp. 373–389.

Kogiso, T., Hirose, K., Takahashi, E., 1998. Melting experiments on homogeneous mixing of peridotitic basalt: application to the genesis of ocean island basalts. Earth Planet. Sci. Lett. 162, 45–61.

Kurz, M.D., Kammer, D.P., 1991. Isotopic evolution of Mauna Loa volcano. Earth Planet. Sci. Lett. 103, 257–269.

Kurz, M.D., Jenkins, W.J., Hart, S.R., Clague, D., 1983. Helium isotopic variations in volcanic rocks from Loihi Seamount and the Island of Hawaii. Earth Planet. Sci. Lett. 66, 388–406.

Kurz, M.D., Garcia, M.O., Frey, F.A., O'Brien, P.A., 1987. Temporal helium isotopic variations within Hawaiian volcanoes: basalts from Mauna Loa and Haleakala. Geochim. Cosmochim. Acta 51, 2905–2914.

Kurz, M.D., Kenna, T.C., Kammer, D.P., Rhodes, J.M., Garcia, M.O., 1995. Isotopic evolution of Mauna Loa Volcano: a view from the submarine southwest rift zone. In: Rhodes, J.M., Lockwood, J.P. (Eds.), Mauna Loa Revealed. AGU, Washington, pp. 289–306.

Kurz, M.D., Kenna, T.C., Lassiter, J.C., DePaolo, D.J., 1996. Helium isotopic evolution of Mauna Kea volcano: first results from the 1-km drill core. J. Geophys. Res. 101, 11781–11791.

Kurz, M.D., Curtice, J., Lott III, D.E., 2004. Rapid helium isotopic variability in Mauna Kea shield lavas from the Hawaiian Scientific Drilling Project. Geochem. Geophys. Geosyst. 5. doi:10.1029/2002GC000439.

Lassiter, J.C., Hauri, E.H., 1998. Osmium-isotope variations in Hawaiian lavas: evidence for recycled oceanic lithosphere in the Hawaiian plume. Earth Planet. Sci. Lett. 164, 483–496.

Lassiter, J.C., DePaolo, D.J., Tatsumoto, M., 1996. Isotopic evolution of Mauna Kea volcano: results from the initial phase of the Hawaiian Scientific Drilling Project. J. Geophys. Res. 101, 11769–11780.

Lipman, P.W., Sisson, T.W., Ui, T., Naka, J., Smith, J.R., 2002. Ancestal submarine growth of Kilauea volcano and instability of its south flank. In: Takahashi, E., Lipman, P.W., Garcia, M.O., Naka, J., Aramaki, S. (Eds.), Hawaiian Volcanoes, Deep Underwater Perspectives. Geophysical Monograph, vol. 128, pp. 161–191.

Malahoff, A., Woollard, G.P., 1968. Magnetic and tectonic trends over the Hawaiian Ridge. In: Knopoff, L., Drake, C.L., Hart, P.J. (Eds.), American Geophysical Union Monograph, vol. 15, pp. 241–276.

Matsuda, J., Matsumoto, T., Sumino, H., Nagao, K., Yamamoto, J., Miura, Y., Kaneoka, I., Takahata, N., Sano, Y., 2002. The $^{3}He/^{4}He$ ratio of the new internal He Standard of Japan (HESJ). Geochem. J. 36, 191–195.

Moore, J.G., Campbell, J.F., 1987. Age of tilted reefs, Hawaii. J. Geophys. Res. 92, 2641–2646.

Moore, J.G., Clague, D.A., Ludwig, K.R., Mark, R.K., 1990. Subsidence and volcanism of the Haleakala Ridge, Hawaii. J. Volcanol. Geotherm. Res. 42, 273–284.

Moreira, M., Breddam, K., Curtice, J., Kurz, M.D., 2001. Solar neon in the Icelandic mantle: new evidence for an undegassed lower mantle. Earth Planet. Sci. Lett. 185, 15–23.

Naka, J., Team, 2000. Tectono-magmatic processes investigated at deep-water flands of Hawaiian volcanoes. EOS Trans. 81 (221), 226–227.

Okano, O., Tatsumoto, M., 1996. Petrogenesis of ultramafic xenoliths from Hawaii inferred from Sr, Nd, and Pb isotopes. In: Basu, A., Hart, S.R. (Eds.), Earth Processes, Reading the Isotopic Code. AGU, Washington, pp. 135–147.

Porcelli, D., Wasserburg, G.J., 1995. Mass transfer of helium, neon, argon, and xenon through a steady-state upper mantle. Geochim. Cosmochim. Acta 59, 4921–4937.

Poreda, R.J., Farley, K.A., 1992. Rare gases in Samoan xenoliths. Earth Planet. Sci. Lett. 113, 129–144.

Ren, Z.-Y., Takahashi, E., Orihashi, Y., Johnson, K.T.M., 2004. Petrogenesis of tholeiitic lavas from the submarine Hana Ridge, Haleakala volcano, Hawaii. J. Petrol. 45, 2067–2099.

Ren, Z.-Y., Ingle, S.S., Takahashi, E., Hirano, N., Hirata, T., 2005. The chemical structure of the Hawaiian mantle plume. Nature 436, 837–840.

Ren, Z.-Y., Shibata, T., Yoshikawa, M., Johnson, K.T.M., Takahashi, E., 2006. Isotope compositions of the submarine Hana Ridge lavas, Haleakala volcano, Hawaii: implications for source compositions, melting process and the structure of Hawaiian plume. J. Petrol. 47, 255–275.

Renne, P.R., Swisher, C.C., Deino, A.L., Karner, D.B., Owens, T.L., DePaolo, D.J., 1998. Intercalibration of standards, absolute ages and uncertainties in $^{40}Ar/^{39}Ar$ dating. Chem. Geol. 145, 117–152.

Rison, W., Craig, H., 1983. Helium isotopes and mantle volatiles in Loihi Seamount and Hawaiian Island basalts and xenoliths. Earth Planet. Sci. Lett. 66, 407–426.

Roden, M.F., Trull, T., Hart, S.R., Frey, F.A., 1994. New He, Nd, Pb, and Sr isotopic constraints on the constitution of the Hawaiian plume: results from Koolau Volcano, Oahu, Hawaii, USA. Geochim. Cosmochim. Acta 58, 1431–1440.

Roy-Barman, M., Wasserburg, G.J., Papanastassiou, D.A., Chaussidon, M., 1998. Osmium isotopic compositions and Re–Os concentrations in sulfide globules from basaltic glasses. Earth Planet. Sci. Lett. 154, 331–347.

Sarda, P., Staudacher, T., Allègre, C.J., 1988. Neon isotopes in submarine basalts. Earth Planet. Sci. Lett. 91, 73–88.

Sleep, N.H., 1990. Hotspots and mantle plumes: some phenomenology. J. Geophys. Res. 95, 6715–6736.

Smith, J.R., Sateke, K., Morgan, J.K., Lipman, P.W., 2002. Submarine landslides and volcanic features on Kohala and Mauna Kea volcanoes and the Hana Ridge, Hawaii. In: Takahashi, E., Lipman, P.W., Garcia, M.O., Naka, J., Aramaki, S. (Eds.), Hawaiian Volcanoes, Deep Underwater Perspectives. Geophysical Monograph, vol. 128, pp. 11–28.

Sobolev, A.V., Hofmann, A.W., Sobolev, S.V., Nikogosian, I.K., 2005. An olivine-free mantle source of Hawaiian shield basalts. Nature 434, 590–597.

Staudigel, H., Zindler, A., Hart, S.R., Leslie, T., Chen, C.-Y., Clague, D., 1984. The isotope systematics of a juvenile intraplate volcano: Pb, Nd, and Sr isotope ratios of basalts from Loihi Seamount, Hawaii. Earth Planet. Sci. Lett. 69, 13–29.

Stille, P., Unruh, D.M., Tatsumoto, M., 1986. Pb, Sr, Nd, and Hf isotopic constraints on the origin of Hawaiian basalts and evidence for a unique mantle source. Geochim. Cosmochim. Acta 50, 2303–2319.

Stolper, E.M., DePaolo, D.J., Thomas, D.M., 1996. Introduction to special section:Hawaii Scientific Drilling Project. J. Geophys. Res. 101, 11593–11598.

Takahashi, E., Nakajima, K., 2002. Melting process in the Hawaiian plume: an experimental study. In: Takahashi, E., Lipman, P.W., Garcia, M.O., Naka, J., Aramaki, S. (Eds.), Hawaiian Volcanoes, Deep Underwater Perspectives. Geophysical Monograph, vol. 128, pp. 403–418.

Takahashi, E., Lipman, P.W., Garcia, M.O., Naka, J., Aramaki, S., 2002. Hawaiian volcanoes: deep underwater perspective. Geophysical Monograph, vol. 128. American Geophysical Union, Washington, D.C. 418 pp.

Tanaka, R., Nakamura, E., 2002. Geochemical evolution of Koolau Volcano, Hawaii. In: Takahashi, E., Lipman, P.W., Garcia, M.O., Naka, J., Aramaki, S. (Eds.), Hawaiian Volcanoes, Deep Underwater Perspectives. Geophysical Monograph, vol. 128, pp. 311–332.

Thirlwall, M.F., 1997. Pb isotopic and elemental evidence for OIB derivation from young HIMU mantle. Chem. Geol. 139, 51–74.

Tilling, R.I., Dvorak, J.J., 1993. Anatomy of a basaltic volcano. Nature 363, 125–133.

Trieloff, M., Kunz, J., Clague, D.A., Harrison, D., Allègre, C.J., 2000. The nature of pristine noble gases in mantle plumes. Science 288, 1036–1038.

Trieloff, M., Kunz, J., Allègre, C.J., 2002. Noble gas systematics of the Reunion mantle plume source and the origin of primordial noble gases in Earth's mantle. Earth Planet. Sci. Lett. 200, 297–313.

Valbracht, P.J., Staudigel, H., Honda, M., McDougall, I., Davies, G.R., 1996. Isotopic tracing of volcanic source regions from Hawaii: decoupling of gaseous from lithophile magma components. Earth Planet. Sci. Lett. 144, 185–198.

Valbracht, P.J., Staudacher, T., Malahoff, A., Allègre, C.J., 1997. Noble gas systematics of deep rift zone glasses from Loihi Seamount, Hawaii. Earth Planet. Sci. Lett. 150, 399–411.

Vance, D., Stone, J.O.H., O'Nions, R.K., 1989. He, Sr and Nd isotopes in xenoliths from Hawaiian and other oceanic islands. Earth Planet. Sci. Lett. 96, 147–160.

Wagner, T.P., Clague, D.A., Hauri, E.H., Grove, T.L., 1998. Trace element abundances of high-MgO glasses from Kilauea, Mauna Loa and Haleakala Volcanoes, Hawaii. Contrib. Mineral. Petrol. 131, 13–21.

West, H.B., Leeman, W.P., 1987. Isotopic evolution of lavas from Haleakala Crater, Hawaii. Earth Planet. Sci. Lett. 84, 211–225.

Wright, T.L., Shaw, H.R., Tilling, R.I., Fiske, R.S., 1979. Origin of hawaiian tholeiitic basalt: a quantitative model. Hawaii Symposium on Intraplate Volcanism and Submarine, p. 104.

Yasuda, A., Fujii, T., Kurita, K., 1994. Melting phase relations of an anhydrous mid-ocean ridge basalt from 3 to 20 Gpa: implications for the behaviour of subducted oceanic crust in the mantle. J. Geophys. Res. 99, 9401–9414.

Yaxley, G.M., Green, T.H., 1998. Reactions between eclogite and peridotite: mantle refertilisation by subduction of oceanic crust. Schweiz. Mineral. Petrogr. Mitt. 78, 243–255.